Decolorization and biodegradability of a real pharmaceutical wastewater treated by H_2O_2-assisted photoelectrocatalysis on TiO_2 meshes

Maria Cristina Collivignarelli[a], Alessandro Abbà[b], Marco Carnevale Miino[a,*], Hamed Arab[c], Massimiliano Bestetti[c], Silvia Franz[c].

[a]: Department of Civil Engineering and Architecture, University of Pavia, via Ferrata 1, 27100 Pavia, Italy

[b]: Department of Civil, Environmental, Architectural Engineering and Mathematics, University of Brescia, via Branze 43, 25123 Brescia, Italy

[c]: Department of Chemistry, Materials and Chemical Engineering "Giulio Natta", Politecnico di Milano, Via Mancinelli 7, 20131 Milano, Italy

(*) Corresponding author: marco.carnevalemiino01@universitadipavia.it; phone number: +39 0382 985311 (Marco Carnevale Miino)

ORCID:

M.C. Collivignarelli (0000-0002-0497-9354)

A. Abbà (0000-0002-1377-9741)

M. Carnevale Miino (0000-0003-3669-1635)

M. Bestetti (0000-0003-2528-2852)

Abstract:

In recent years, photoelectrocatalysis (PEC) for the treatment of industrial wastewaters (IWWs) has been repeatedly proposed. However, despite the number of tests reported in literature, only a few of them were conducted on real IWWs. In this study, real pharmaceutical IWWs showing an intense recalcitrant color were treated by PEC and H_2O_2-assisted PEC (UV/TiO_2/Bias and UV/H_2O_2/TiO_2/Bias, respectively) on TiO_2 meshes having sub-micrometric features obtained by Plasma Electrolytic Oxidation. Photolysis (UV), chemical oxidation (H_2O_2) and H_2O_2-assisted photolysis (UV/H_2O_2) were tested in the same reactor for comparison. The configuration UV/H_2O_2/TiO_2/bias showed the best results in term of decolorization efficiency and rate, where decolorization was 55% (single-step H_2O_2 dosing) and 44% (three-step H_2O_2

dosing), after 2h of contact time. In the same contact time, UV and UV/TiO_2/Bias processes did not give decolorization. A more effective COD removal was measured for the PEC processes, UV/H_2O_2/TiO_2/Bias (-24%) and UV/TiO_2/Bias (-20%), while COD removal by UV was almost 0%. Correspondingly, the SOUR values showed that PEC combined with a single-step H_2O_2 dosage was the most effective configuration, leading to the highest biodegradability of the treated IWW with respect to the other processes. The energy consumption analysis demonstrated that PEC+H_2O_2 (single-step dosage) optimized energy costs.

Keywords: pharmaceutical wastewater, AOPs, electrochemical processes, photoelectrocatalysis, titanium dioxide

1. Introduction

The treatment of real wastewaters requires to simultaneously address several issues, such as decolorization (Collivignarelli et al., 2017b; Dotto et al., 2019) and presence of surfactants (Freeling et al., 2019), pharmaceuticals (Zhan et al., 2019) and heavy metals (Collivignarelli et al., 2019a). In recent years, the release of colored wastewater (WW) into the environment became a significant problem. Indeed, dyes can have a negative aesthetic impact (Maiti et al., 2017), increase pollution in environment, altering the balance of flora and fauna (Mashkoor et al., 2018) and potentially have negative effects on human health such as skin irritation, respiratory problems, mental disorder and in many cases they may be carcinogenic and mutagenic (Mashkoor et al., 2018; Roy et al., 2018). Among IWWs, effluents from pharmaceutical plants are considered a big source of environmental pollution (Zhan et al., 2019). In recent years much attention has been given to the degradation of pharmaceutical products (Asif et al., 2017; Zhao et al., 2019), but pharmaceutical WWs can present also a strong colorization (Wen et al., 2018). Many treatments for pharmaceuticals degradation have been developed, but only few of them have been tested for color removal and mostly on synthetic WWs.

Among the mostly proposed technologies for color removal from WWs, chemical/physical, chemical (conventional and advanced), electrochemical and biological processes should be mentioned (Cardoso et al., 2016; Collivignarelli et al., 2019b; Liu and Zhu, 2017). However, conventional WWs treatments not always lead to a sufficient decolorization, most of the times because they are not designed to remove color (Robinson et al., 2001). Advanced oxidation processes (AOPs) can be effective in decolorization and can be easily integrated with biological treatments, as they often increase the biodegradability of WWs (Del Moro et al. 2013, Del Moro et al. 2016). Among AOP_S, in the last years, increasing attention was raised by photocatalysis, as often no chemicals are needed and the reactive species produced–by UV irradiation of the catalyst are non-specific (Andronic et al. 2016, Cates 2017). Indeed, the reactive species are radical

53 species $^{\bullet}OH$ having a very high redox potential ($^{\bullet}OH/H_2O$ 2.80 V vs SHE at T_{room}), comparing to other oxidizing agents,
54 such as ozone (O_3/O_2,H_2O 2.07 V) or chlorine (Cl_2/Cl^- 1.36 V) (Collivignarelli et al., 2017a; 2019b). Although an
55 incomplete mineralization could lead to the formation of by-products showing higher toxicity than dyes themselves (Wang
56 et al., 2008), in-principle hydroxyl radicals are able to accomplish a non-selective degradation of any pollutant in the waters,
57 including chromophores (Collivignarelli et al., 2019b).

58 The more common photocatalytic approaches are based on dispersion of TiO_2 sub-micrometric powders in WWs and suffer
59 from low efficiency due to low quantum efficiency and possible catalyst poisoning. Additionally, the recovery of catalyst
60 powders can be difficult and can have a significant impact on the overall cost of the process. Such issue can be overcome
61 by immobilization of the TiO_2 particles on substrates (Murgolo et al., 2017). However, this approach does not improve the
62 quantum efficiency and, as a matter of fact, the application of photocatalysis based on supported catalytic powders for the
63 treatment of real WWs is still very rare.

64 More recently, photoelectrocatalysis (PEC) was proposed to simultaneously face the issues of catalyst recovery and low
65 quantum efficiency typical of photocatalysis (Cui et al., 2018; Franz et al., 2015; Garcia-Segura and Brillas, 2017;
66 Suhadolnik et al., 2019; Wang et al., 2017). In fact, PEC makes use of catalytic films deposited onto conductive substrates
67 and allows the reduction of the recombination of photogenerated electronic species due to the application of a positive bias
68 to the photoanode during operation. The nature and properties of the photoanode are very important because a series of
69 oxidation reactions take place at its surface. Titanium dioxide (TiO_2) is commonly used to produce photoanodes (Wang et
70 al., 2018). Indeed, TiO_2 shows many advantages such as high photoactivity, good chemical and thermal stability, low
71 environmental impact and low cost (Komtchou et al., 2016; Nakata and Fujishima 2012, Zhang et al., 2018). Photoactive
72 TiO_2 coatings can be synthesized by a number of techniques including sol-gel, CVD, RF magnetron sputtering, plasma
73 spray, e-beam evaporation and annealing, anodic oxidation (AO) (Bestetti et al. 2007) and plasma electrolytic oxidation
74 (PEO) (Franz et al. 2016). In the cases of AO and PEO, the photoactive coating grown directly on titanium substrates shows
75 good mechanical adhesion to the substrate and good electrical conductivity. PEO shows several technological advantages
76 over AO. Indeed, the high operating voltage applied during PEO induces high growth rates (~ 1 μm/min), instantaneous
77 oxide crystallization and incorporation of chemical species from the electrolyte (Yerokhin et al. 1999, Franz et al. 2016,
78 Mirelman et al. 2012). PEO process is an industrial technology used to synthesize protective layers on aluminum and
79 magnesium alloys (Yerokhin et al. 1999), and titanium alloys, mostly Ti-6Al-4V for biomedical implants (Yerokhin et al.
80 2000).

As for the technological advantages, PEC itself is a promising approach as it can benefit of the consolidated background of the industry in the design of UV plants, where photoanodes could be easily integrated.

Photoanodes obtained by PEO already showed to be effective in the degradation of model dyes (Franz et al. 2015). More recently, some of the authors demonstrated that PEC based on photoanodes made by PEO is effective in the degradation of emerging organic pollutant (Murgolo et al., 2019). In the same paper, it was also clearly showed that the high efficiency of the PEC process could be attributed to due to a synergistic effect with UV light and electrical polarization, leading to a faster degradation kinetics with respect to both UV light + catalysts process or the electrochemical process. Moreover, PEC does not produce sludge, minimizing the production of secondary waste, as requested by European Directive 2018/851 (Collivignarelli et al., 2019 c,d). Despite these very promising results, PEC is not yet an industrial technique for the treatment of real WWs.

In the present study, the authors apply PEC based on PEO photoanodes to the treatment of pharmaceutical WWs showing an intense recalcitrant color. Both PEC and PEC with addition of hydrogen peroxide were studied. Photolysis (UV) and chemical oxidation (H_2O_2) were tested in the same reactor for comparison. In addition to color removal, other parameters such as BOD_5, COD and SOUR were monitored. Finally, the energy consumption in relation to COD and color removal was calculated.

2. Materials and Methods

2.1. Materials

2.1.1. Chemical analysis of the industrial wastewater

In the tests a real pharmaceutical IWW was used whose characteristics are reported in Table 1. The company, from which the IWW has been collected, produces chiral materials (high-value amino acids) as starting materials and intermediates products for the pharmaceutical industry. It also manufactures materials for the cosmetic industries and related compounds. The IWW is characterized by high value of COD (up to 1900 mg L-1), low biodegradability and strong dark orange colorization (Figure S1).

Table 1: *Chemical and biochemical properties of the IWW.*

Parameter	**u.m.** [(b)]	**Value**
Measured		
AB_{254} [(a)]	A.U.	8.3 - 8.8

COD	mg L^{-1}	1600 - 1900
TOC	mg L^{-1}	580 - 610
pH	-	7.8 - 8.0
EC [(c)]	mS cm^{-1}	11.0 - 11.2
BOD_5	mg L^{-1}	450 - 500
Calculated		
k [(d)]	d^{-1}	0.301 – 0.360
I_{biod} [(e)]	%	27 - 31
Ir_{biod} [(f)]	%	81 - 84
SOUR	$mgO_2\ g_{VSS}^{-1}\ h^{-1}$	4.6 - 5.8

(a) AB_{254}: value of absorbance at 254 nm of wavelength

(b) u.m.: unit of measure

(c) EC: electrical conductivity

(d) k: rate of biodegradation

(e) I_{biod}: biodegradability index

(f) Ir_{biod}: rapidity of biodegradation index

Temperature, pH and conductivity were measured using a portable multiparameter instrument (WTW 3410 SET4). Electrical conductivity was measured using the probe WTW-IDS, model TetraCon® 925. Temperature and pH were measured using the probe WTW-IDS, Model SenTix® 940. During the decolorization tests, the absorbance spectra of the samples in range from 190 to 820 nm was measured by UV/Vis spectrophotometry (HP 8453 spectrophotometer).

2.1.2. Synthesis and characterization of the TiO_2 films

A mesh of commercially pure Grade 1 titanium mesh (400 cm^2) was treated by Plasma Electrolytic Oxidation (PEO) in a 1.5 M H_2SO_4 aqueous solution, following the approach described by Franz et al. (2016). The PEO cell voltage was set at 150 V for 5 minutes, and the electrolyte temperature at about -5 °C by using a cryostat (HAAK D10). Right after PEO, the oxidized mesh was rinsed with water and dried in a stream of air. A Scanning Electron Microscopy (SEM - Zeiss EVO 50), and an X-ray diffraction (XRD - Philips PW1830) instruments were used to investigate morphology and phase

structure of the obtained TiO_2, respectively. As shown in Figure 1, the oxide layer was porous with sponge-like morphology, which enhanced the effective surface area for photoelectrochemical applications. As shown in Figure 1, the as-grown TiO_2 film had a crystalline structure consisting in a mixture of the two allotropes anatase and rutile. Based on Spurr and Myers (1957), the mass fractions of anatase and rutile phases were estimated to be about 58 % and 42 %, respectively. The thickness of the TiO_2 film was assessed by Glow Discharge Optical Emission Spectrometry (GD-OES) using a Spectrum GDA750 analyzer operated at 700 V in argon atmosphere at 230 Pa. The GD-OES in depth profile of the Titanium and Oxygen elements (not shown) revealed that the thickness of the grown TiO_2 is around 2 μm.

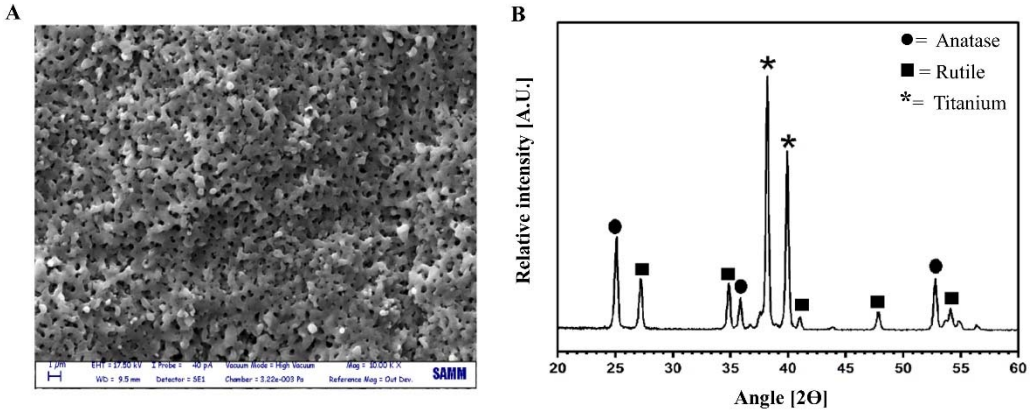

Figure 1: ***(A)*** *SEM surface micrograph of the TiO_2 film;* ***(B)*** *XRD pattern of as-grown TiO_2 film. (COLOR online only) (2-column fitting image)*

2.1.3. Laboratory scale reactor

The tests were conducted in semi-batch mode. In Figure 2A the scheme of the hydraulic circuit of the system is shown. The wastewater was introduced into a 2.4 L tank at the bottom of the machine and, by means of a pump (Iwaky Magnet Pump MD-30RZ-220N with 80 kW of nominal power), it was pumped into the reactor, having a volume of 1 L. From this inlet point, the IWW was recirculated to the initial tank. The water samples for analysis were collected from a tap placed at the bottom of the tank. During the tests, the apparatus was hermetically closed. As shown in Figure 2B, the IWW was pumped upward through the reactor. At the center axis of the reactor, a 30 W medium-pressure Hg vapor lamp was arranged. The radiance flux density under the different reactor configurations (see Section 2.2.1) was measured by actinometry test by using 10 μM Uridine (Sigma-Aldrich). The anodized titanium mesh was coaxially surrounding the UV lamp with a gap of few millimeters. The geometrical surface area of the TiO_2 catalyst was around 327.5 cm^2. Since

surface enhancement was expected due to porosity, real surface area measurements were carried out. Surface area was evaluated by low temperature (77 K) N_2 adsorption using a Tristar II 3020 Micromeritics apparatus after outgassing the samples at 80°C for 24 h under nitrogen flux. Based on the nitrogen isotherms using BET theory from the instrumental software (Version 1.03), the surface area of the catalyst was 6,6 $m^2 g^{-1}$. Additionally, further characterization of the surface area was carried out by electrochemical methods. In particular, Electro-Chemical Surface Area (ECSA) measurements were carried out by measuring the capacitance by performing cyclic voltammetry at different scan rate in the non-faradaic region around the open-circuit potential value (Trasatti and Petrii, 1992). The estimated ECSA was 5.7 $m^2 g^{-1}$ for the TiO_2 film. Considering the different phenomena accounting for the ECSA test, the values obtained can be considered in good agreement with the BET surface value. Based on the ECSA value, the total electrochemical surface area of the catalyst was 1.795 m^2. During the PEC tests, the anodized titanium mesh was anodically polarized while the reactor body was cathodically polarized. A constant cell voltage of 4V was applied by means of a potentiostat/galvanostat (AMEL 2549). The same instrument allowed continuous chronoamperometric monitoring of the photoelectrochemical activity of the TiO_2 mesh. The flow rate in the system was kept constant at 700 L h^{-1}. To quantify the effect of the anodized mesh on the UV dosage provided to the WWs, actinometric measurements were carried out. H_2O_2 has been purchased from Sigma-Aldrich Corp. (PCode: 101896237; Concentration: 30 % w/w).

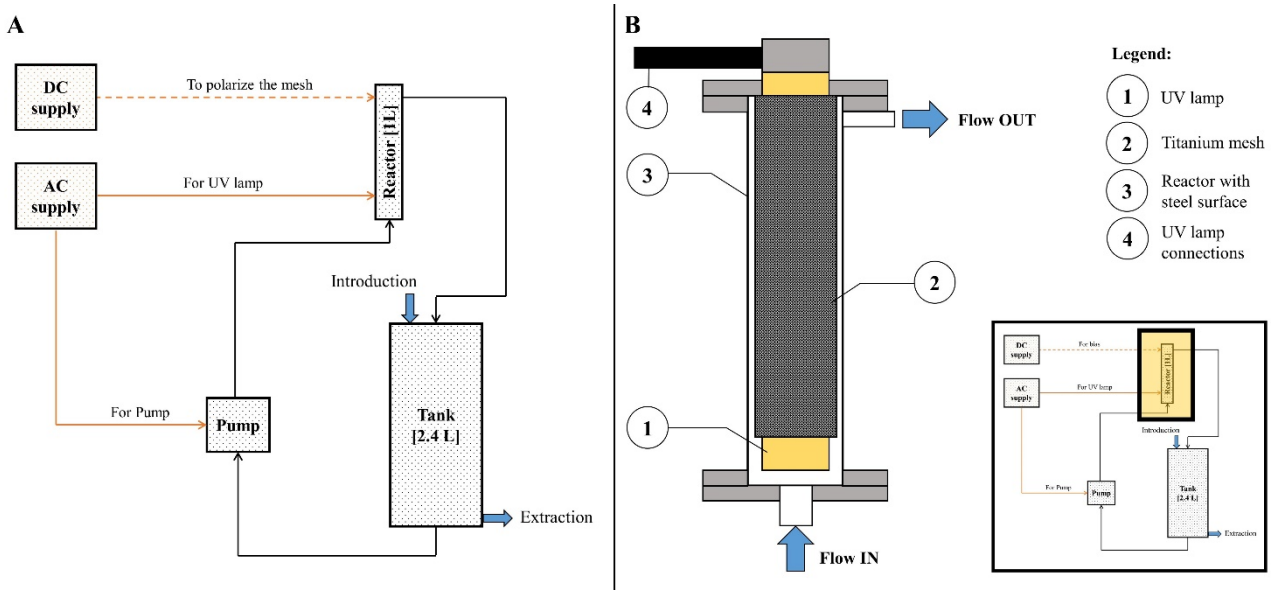

Figure 2: *(**A**) Schematic of the hydraulic circuit; (**B**) Schematic of the laboratory-scale electrochemical photoreactor working in up-flow condition and semi-batch mode. (COLOR online only) (2-column fitting image).*

2.2. Methods

2.2.1. Decolorization tests

Five different working conditions were tested:

A) UV (photolysis)

B) H_2O_2 (50 mg L^{-1}; 200 mg L^{-1}; 500 mg L^{-1}; 1500 mg L^{-1}; 3000 mg L^{-1} per single dose)

C) UV/H_2O_2 (1500 mg L^{-1} per single dose)

D) UV/TiO_2/bias 4V (PEC)

E) UV/TiO_2/bias 4V + H_2O_2 (1500 mg L^{-1}, single-step dosage) (H_2O_2-assisted PEC)

F) UV/TiO_2/bias 4V + H_2O_2 (1500 mg L^{-1}, three-steps dosage 500 mg L^{-1} each) (H_2O_2-assisted PEC)

The different tests were carried out for the time needed to observe decolorization. Tests A, C and D were carried out for a contact time of 57.5 h, tests B for 3 h, tests E and F were carried out for a contact time of 2 h. Each test was replicated to assess the reliability of the results. Taking into account that the reactor was working in a semi-batch mode, processing time has been converted into contact time considering the following equation (Eq.1):

$$Contact\ time = processing\ time * \frac{V_R}{V_S} \quad (1)$$

where V_R is the volume of the reactor (1L) and V_S is the total instantaneous volume circulating in the system.

During the treatment, several samples were collected, whose absorbance at IWW characteristic wavelengths (474 nm), COD and BOD_5 were measured. Furthermore, during the PEC tests, pH and electrical conductivity of the matrix were monitored.

2.2.2. Analysis of the IWW

BOD_5, COD, and H_2O_2 concentration were measured according to the *standard methods for the Examination of water and wastewater* (APHA, 2012). For the analysis, Hack kits have been used. Before the COD analysis, the interference from chlorides was ruled out by verifying that the chloride concentration was lower than the maximum accepted by the method.

177 The color analysis was performed following the *Standard Methods for the Examination of Water and Wastewater* (APHA,
178 2012). After identifying the characteristic wavelength of the sample, the decolorization was calculated as reported in Eq.2:

179 $$Decolorization = \frac{(A_0 - A_i)}{A_0} * 100 \quad (2)$$

180 Where A_0 is the initial absorbance at the characteristic wavelength of the sample and A_i is the currently i-th absorbance
181 at the characteristic wavelength of the sample. According to the APHA method (APHA, 2012), the characteristic
182 wavelength of the specific IWW considered in the present investigation was 474 nm.

183 The BOD_{TOT} [mg L^{-1}] and the rate of biodegradation k [d^{-1}] were calculated following Fujimoto (1964), Gotovtsev (2016)
184 and Oke et al. (2018). The biodegradability index (I_{biod}) and the rapidity of biodegradation index (Ir_{biod}) were calculated
185 according to Eq.3 and Eq.4, respectively:

186 $$I_{biod} = \frac{BOD_{TOT}}{COD} * 100 \quad [\%] \quad (3)$$

187 $$Ir_{biod} = \frac{BOD_5}{BOD_{TOT}} * 100 \quad [\%] \quad (4)$$

188 Specific Oxygen Uptake Rate (SOUR) tests were carried out at 20 °C adopting the ISO 8192 procedure (ISO 8192, 2007),
189 using a mesophilic biomass withdraw from a wastewater treatment plant (authorized to treat municipal wastewater and
190 aqueous waste) at different times during the UV, PEC and H_2O_2-assisted PEC processes. These tests aimed to evaluate
191 the suitability of the treated IWW to be recirculated into a mesophilic biological treatment (Collivignarelli et al., 2019c).
192 This aspect is very important, in order to evaluate the effects on the mesophilic biomass of a centralized activated sludge
193 treatment plant, when the effluent of the pharmaceutical company is discharged into a public sewer system (Collivignarelli
194 et al., 2014).

195 **2.2.3. Energy consumption**

196 According to literature (Bessegato et al., 2018; Cardoso et al., 2016; Malpass et al., 2007), the efficiency of
197 electrochemical process can be evaluated according to the kinetic model describing the system under investigation. Given
198 the high COD concentration, the removal rate can be considered phenomenologically *zero order*. Therefore, the rate of
199 removal of this contaminant has been considered directly proportional to the rate of electric energy use (Bolton et al.,

200 2001). Therefore, the energy consumption has been calculated as Electrical energy per unit of mass (E_{EM}) in [kW h Kg^{-1}]
201 with the following equation (Eq. 5) (Bolton et al., 2001):

202 $$E_{EM} = \frac{P*t*10^6}{V*(\gamma_i-\gamma_f)}\ [kW\ h\ Kg^{-1}] \quad (5)$$

203 where P is the nominal power [kW] of the system, t [h] is the processing time, V [L] is the volume of water treated and γ
204 represents the concentration of COD in [mg L^{-1}]. The nominal power (P) was assumed equal to the sum of the individual
205 energy consumption of the pump, the lamp and the power supply for PEC process.

206 Following Malpass et al. (2007), energy consumption was also correlated with color removal as Electrical energy per
207 order (E_{EO}) in [kW m^{-3} $order^{-1}$], according to Eq. 6 (Bessegato et al., 2018; Bolton et al., 2001):

208 $$E_{EO} = \frac{P*t*10^3}{V*\log_{10}\left(\frac{C_i}{C_f}\right)}\ [kW\ h\ m^{-3}\ order^{-1}] \quad (6)$$

209 where P [kW], t [h] and V [L] have the same definition as in Eq. 5 and C represents the absorbance of samples [A.U.]. In
210 the present study, it was assumed that the amount of electric energy required to bring a reduction by one order of
211 magnitude in color is independent of initial color. This approximation can be used when the concentration of contaminants
212 is low (Bolton et al., 2001; Cardoso et al., 2016; Malpass et al., 2007). E_{EM} and E_{EO} were evaluated after 20 min and 2h
213 of contact time, corresponding to 1h and 6h of processing time, respectively.

214 ## 3. Results and discussion

215 ### 3.1. Photolysis and photoelectrocatalysis

216 Color removal from the IWW showed different features depending on the applied process. Figure 3 shows that UV and
217 UV/TiO_2/bias treatment resulted in decolorization yields of about 50% after a relatively long contact time, i.e. 25h by UV
218 and 45h by UV/TiO_2/bias, with color recrudescence within the first 13.5h and 35h, respectively. However, it was also
219 observed that after 57.5h PEC showed to be more effective than UV process. The pH and electrical conductivity (EC)
220 were also monitored during all tests. During tests, the values did not significantly change, remaining at a value of about
221 8 and 11 mS/cm, respectively.

222 In literature the results on decolorization using PEC strongly depend on the targeted chromophores mixture. For instance,
223 it is reported that in 24h contact time the Direct Green 26 (DG 26) can be removed from an ideal matrix (MilliQ water)
224 more effectively by PEC (87.5 %) than by UV alone (40.1 %) (Turolla et al., 2012). Moreover, Hou et al. (2009) showed

that after 3h contact time the Acid Orange II (AOII) removal was 10.7 % by with UV and 23.7 % by PEC. In the case of the real pharmaceutical IWW used in the present study, in the medium term (15-45h) the PEC process showed a lower removal rate than the UV treatment, while the contrary was observed in the long term (>53h). This behavior can be explained by considering two different features: (i) the TiO_2 mesh is positioned in close proximity to the UV lamp, thus significantly shielding the UV radiation; (ii) the catalyst was not effectively photoactivated due to the high absorbance of the IWW at 254 nm. As for the former issue, the anodized mesh was positioned in close proximity of the UV source with the aim of effectively photoactivate the catalyst. However, this also induced a significant UV shielding effect on the treated waters. The shielding effect was quantified by actinometry and consisted in a decrease of UV dosage provided to the water samples by 50 % with respect to photolysis carried out in the same reactor. Based on actinometry tests, the radiance flux density without the mesh was 0.16 W cm^{-2} and decreased to 0.08 W cm^{-2} using the mesh. As for the second issue, the high absorption coefficient of the IWW in the spectral range of catalyst photoactivation inhibited the activation of the catalysts and thus the PEC process overall. To overcome this problem, H_2O_2 was dosed during PEC (please refer to Section 3.3 for further discussion).

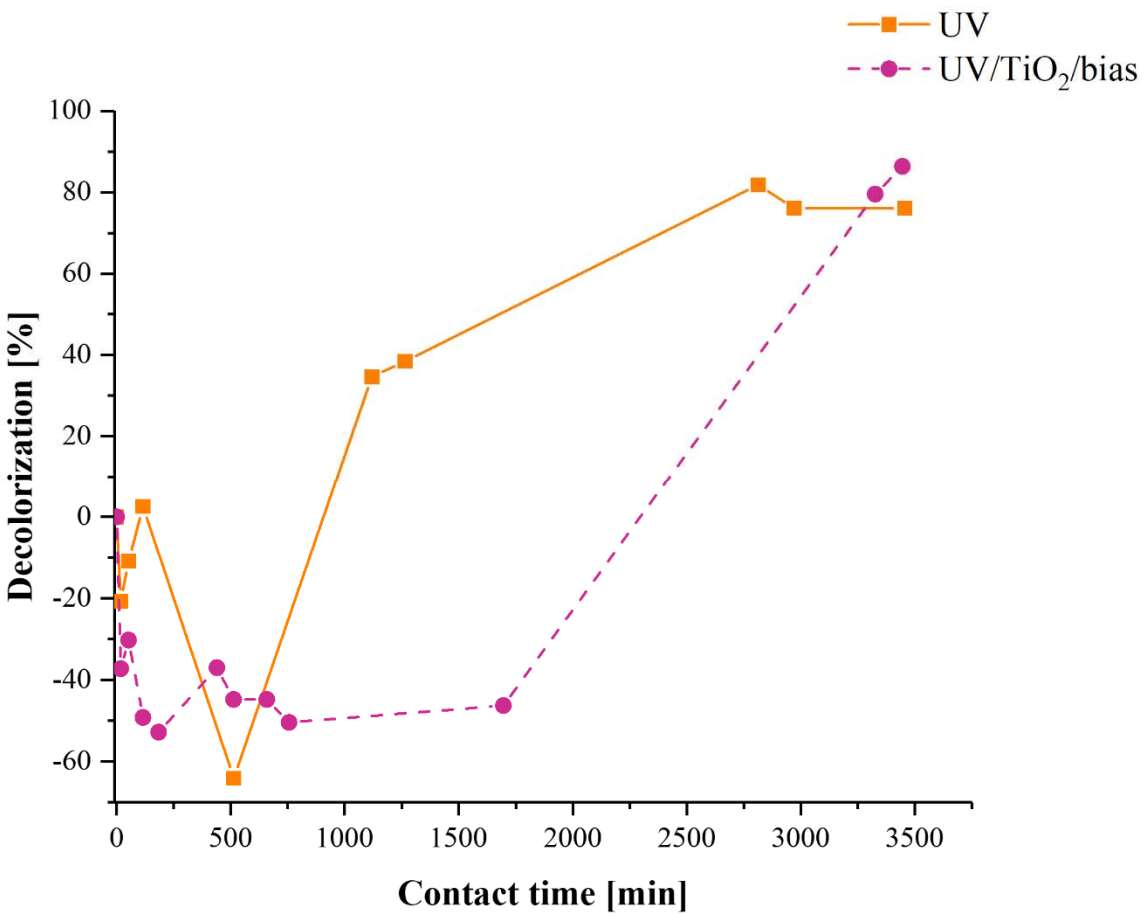

238

239 ***Figure 3:*** *Decolorization of IWW treated by UV and UV/TiO_2/bias (PEC) processes. (COLOR online only) (single column*
240 *fitting image).*

241 As thoroughly reported in literature (Hao et al., 2000), a distinction should be made between color removal and
242 degradation. This means that the concentration of chromophores could also show an anticorrelation with COD values.
243 Figure 4A shows the evolution of decolorization yields compared to COD removal for UV and UV/TiO_2/bias processes.
244 During the UV/TiO_2/bias treatment, COD removal yields were higher than during UV. This tendency culminates after
245 57.5h of contact time, when the COD removal was over 40 % by PEC and only 18 % by UV. However, these COD
246 removal values were much smaller than the corresponding color removal values, which were 76 % and 86 % by UV and
247 PEC, respectively, this discrepancy being particularly pronounced by UV. This divergence can be explained considering
248 that only a small part of COD consists in chromophores. Furthermore, since the discrepancy is more pronounced by UV,
249 being the UV dosage higher than during UV/TiO_2/bias, it can be argued that UV irradiation mainly targets the
250 chromophore functional groups, but it has a limited effect on the degradation of the organic molecules. On the contrary,

the hydroxyl radicals produced during PEC target not only the chromophore parts of the pollutants, but they also cause degradation of the whole molecules.

This also accounts for the anticorrelation between color removal and COD observed at contact times lover than 57,5h. For instance, after 2h of UV treatment, despite a 50 % recoloration the corresponding COD value did not change. Therefore, color recrudescence does not necessarily correspond to an increase in COD. This can be explained considering that the degradation of the matrix can lead to the formation of new intermediate molecules having more active chromophores and causing an even more intense coloration. This is reasonable considering that the matrix was in fact a mix of real pharmaceutical IWW and presented several chromophore-containing molecules.

Although the first phase of this treatments presented a recrudescence of color and not significant yields in COD removal, the biodegradability and the potential treatability of the IWW through a biological process increased significantly (Figure 4B). Performances are different depending on the contact time. After 2h photolysis allowed the higher increase in SOUR (from 5.8 to 16.5 $mgO_2\ g_{VSS}^{-1}\ h^{-1}$) while PEC increases IWW's potential treatability through a biological process only from 4.6 to 9.8 $mgO_2\ g_{VSS}^{-1}\ h^{-1}$. In the medium term, UV treatment proved to be faster also in terms of decolorization yield.

In the long term (after 57.5h of contact time), the SOUR of IWW treated with PEC was almost 50 % less than that of waters treated by photolysis (respectively 12 and 22 $mgO_2\ g_{VSS}^{-1}\ h^{-1}$). Apparently, it might be concluded that the UV process is more effective than PEC both in terms of decolorization and increase in biodegradability. However, it must be taken into account that SOUR measures the aerobic degradation process of organic material (Hagman and La Cour Jansen, 2007) in the same conditions of initial biodegradability, therefore a lower value of COD corresponds to lower SOUR. In the present case, the absolute values of SOUR between UV and PEC cannot be directly compared since the COD values are different. For example, in the medium term (2 h of contact time) the COD value of the IWW was 1918 $mg\ L^{-1}$ after UV and 1139 $mg\ L^{-1}$ after PEC. Although a direct comparison is meaningless, it is worth pointing out that both PEC and UV were able to increase value of SOUR and so the potential treatability of the IWW through a biological process. This observation is particularly of interest for PEC, as literature reports that the biodegradability of IWW treated by photocatalysis onto TiO_2 powders was reduced due to the formation of less biodegradable intermediates and the destruction of the biodegradable compounds in the untreated WW (Stasinakis, 2013). In reverse, in this study the use of polarized TiO_2 meshes having sub-micrometric features clearly favored the formation of short chain biodegradable

intermediates during the oxidation process. In fact, the significant increase in the SOUR values demonstrates the higher biodegradability of IWW after PEC.

Other evidences of the significant increase in biodegradability are reported in Table 2. After 57.5h of contact time, these processes allowed to reach the characteristics of treatability through a biological process. Both the UV and PEC increased the biodegradability index, reducing the length of molecules without affecting the rapidity of biodegradation index. This means that photolysis and PEC can increase not only BOD_{TOT} but also BOD_5. Moreover, the rate of biodegradation (k) increase both for PEC and UV. This symbolizes that the oxygen in the test was consumed with a higher speed and therefore a greater quantity of organic substance has been degraded. Therefore, the strong increase of BOD_5 COD^{-1} must be attributed not only to the reduction of COD value but also to the increase of the BOD_5 value.

Table 2: *COD, rate of biodegradation (k), biodegradability index (I_{biod}) and rapidity of biodegradation index (Ir_{biod}) of the IWW treated by UV and UV/TiO_2/bias after 57.5h of contact time.*

Parameter	**UV** (Δ %)	**UV/TiO_2/bias** (Δ %)
COD [mg L^{-1}]	1570	802
	(- 17.7)	(- 42.1)
BOD_5 COD^{-1} [-]	0.46	0.37
	(+ 76.9)	(+ 68.2)
k [d^{-1}]	0.393	0.325
	(+ 9.2)	(+ 4.8)
I_{biod} [%]	54	48
	(+ 74.2)	(+ 77.8)
Ir_{biod} [%]	86	78
	(+2.4)	(- 3.8)

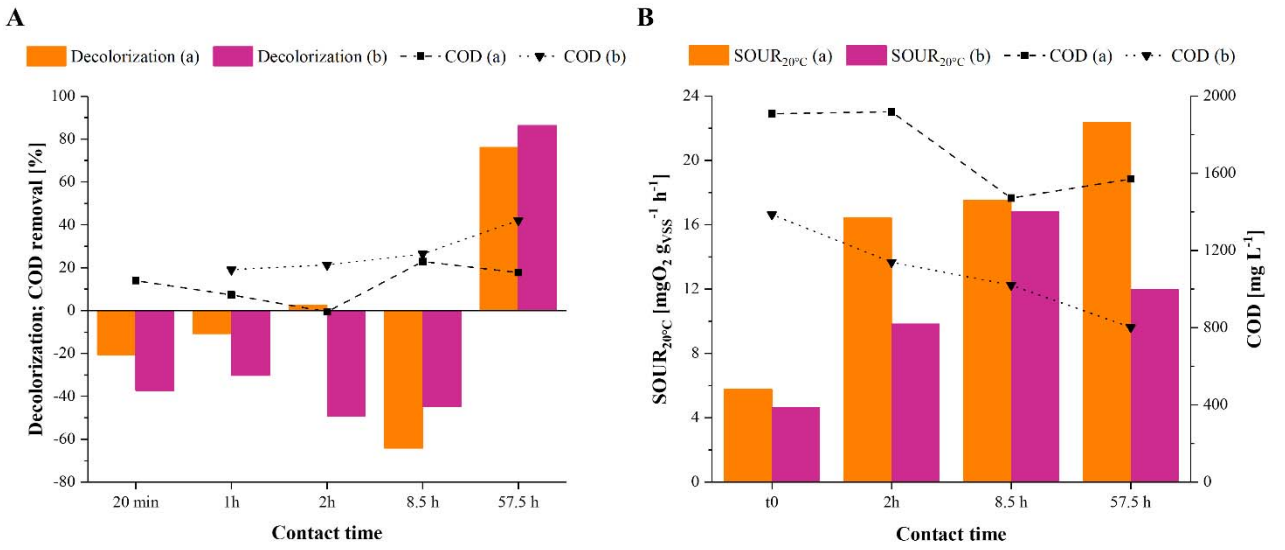

Figure 4: *Decolorization and COD removal* ***(A)****, SOUR and COD values* ***(B)*** *after UV (a) and UV/TiO_2/bias (b) processes as a function of the contact time. (COLOR online only) (single column fitting image).*

3.2. H_2O_2 and H_2O_2-assisted photolysis

As previously mentioned, the low decolorization efficiency observed during the UV/TiO_2/bias process could be attributed to the absorbance spectrum of the IWW under investigation. In order to clarify this point, the correlation between the absorbance of the IWW and the activity of the TiO_2 mesh was investigated. In Figure 5 the absorbance of the IWW at λ= 254 nm is represented as a function of the contact time. Within the first 20 h, the absorbance of the IWW maintained at values ranging from about 7 A.U. to 8 A.U., then it underwent a decreasing trend with an overall reduction of 65% at the end of the process. Correspondingly, in the first stage of the process the current flowing in the photoelectrocatalytic reactor was relatively low (1.7 mA), while it increased to about 37 mA afterwards. It is well-known that the electrical current measured during the PEC process is given by the electrons photoexcited in the conduction band of the catalyst and corresponds to the number of positive vacances left in the valence band, which in turn are responsible for OH• radicals production. Therefore, there is a close correlation between the electrical current circulating in the PEC reactor and the OH• radicals production rate. In order to trigger electrons photopromotion, photons having a suitable wavelength must be delivered to the catalyst surface. Based on crystalline phase composition of the TiO_2 catalyst employed in the present study, the activation wavelength was about 254 nm (Franz et.al. 2016). Since the IWW included chromophores absorbing at 254 nm, the PEC process was initially hindered because of the optical shielding effect given by the IWW itself. Only after photolytic degradation of the chromophores absorbing at 254 nm the PEC process could operate. This is also

consistent with the decolorization yield obtained by PEC in the first stage of the treatment (Figure 3B), where low color removal and/or color recrudescence was observed.

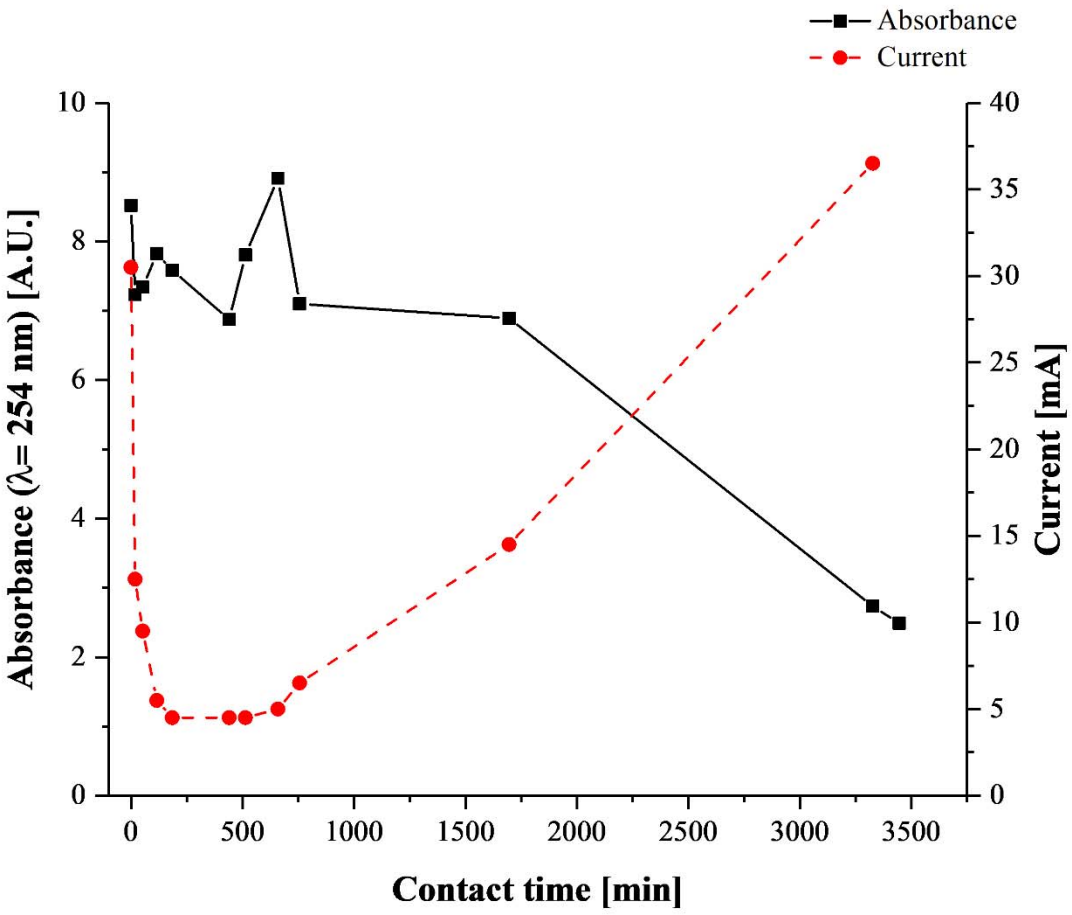

Figure 5: *Photocurrent flowing in the rector during UV/TiO_2/bias process and absorbance values of the IWW, at 254 nm. (COLOR online only) (single column fitting image).*

In order to overcome this problem, the effect of a controlled dosage of H_2O_2 was studied.

Five H_2O_2 concentration values were tested, namely 50 mg L^{-1}, 200 mg L^{-1}, 500 mg L^{-1}, 1500 mg L^{-1} and 3000 mg L^{-1}. After the addition of H_2O_2, the IWW was monitored by spectrophotometry for a total time of 180 min. In Figure 6A, the absorbance of the IWW at λ= 254 nm is represented as a function of the contact time. The Figure shows the effect of the five tested H_2O_2 concentration values on AB_{254}. The value of the AB_{254} was affected both by H_2O_2 dosage and contact time. On average the AB_{254} decreased as the contact time increased. At the same contact time, a higher H_2O_2 dose caused a stronger decrease of the AB_{254} of IWW. Despite H_2O_2 alone did not allow high yields of color removal (10-15 %, Figure

6B), it reduced the color recrudescence especially using the higher dosages. Taking these aspects into account, the dosage of 1500 mg L^{-1} H_2O_2 (H_2O_2 $COD_{initial}^{-1}$ ratio= 0.8) has been selected as the optimal solution both for reducing AB_{254} and minimizing color recrudescence in the UV/TiO_2/bias process. In fact, a higher dosage of H_2O_2 (e.g. 3000 mg L^{-1}) did not lead to better results in terms of color removal and AB_{254} reduction. None of the tested H_2O_2 dosages were able to determine a COD removal (data not shown).

Furthermore, in order to exclude that the decolorization in H_2O_2-assisted PEC assisted was attributable only to the combined presence of UV and H_2O_2, UV/H_2O_2 [1500 mg L^{-1}] has been tested. As reported in Figure 6C, the decolorization and COD removal after 57.5 h were 80% and 35%, respectively (6% and 7% lower, respectively, then those obtained after UV/TiO_2/bias process (Figure 4A)). These results are in agreement with literature, where it is shown that UV/H_2O_2 is less effective than photocatalysis and H_2O_2 assisted-photocatalysis in terms of color and COD removal (Arslan et al., 2000; Garcia et al., 2007).

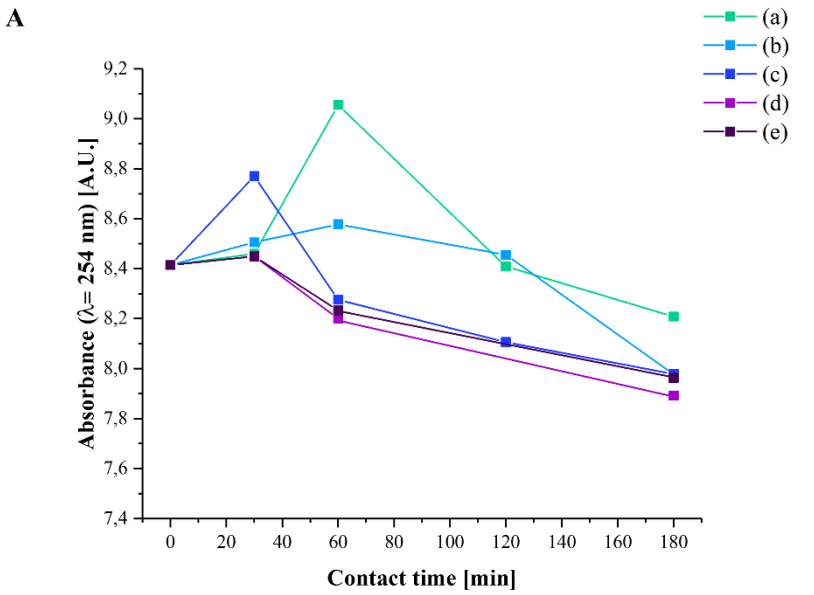
A
(a)
(b)
(c)
(d)
(e)
Absorbance (λ= 254 nm) [A.U.]
9,2
9,0
8,8
8,6
8,4
8,2
8,0
7,8
7,6
7,4
0
20
40
60
80
100
120
140
160
180
Contact time [min]

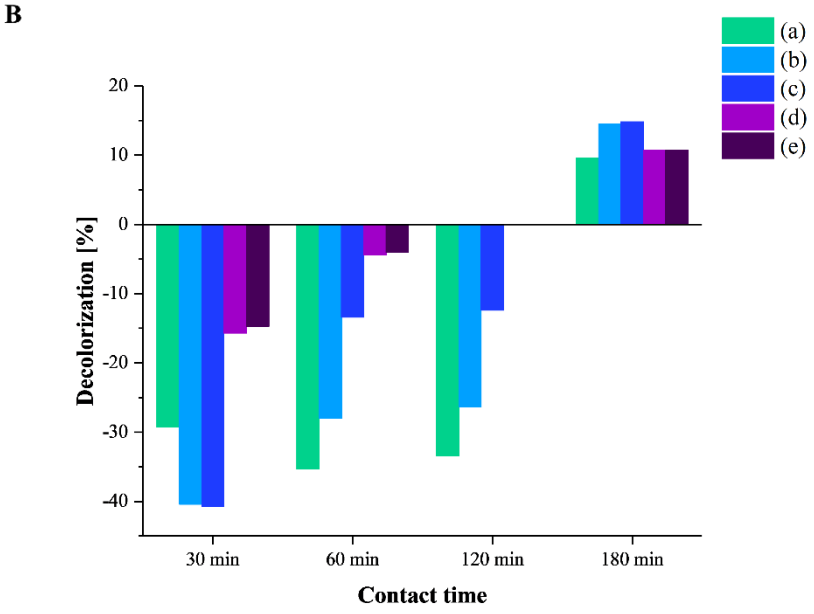
B
(a)
(b)
(c)
(d)
(e)
Decolorization [%]
20
10
0
-10
-20
-30
-40
30 min
60 min
120 min
180 min
Contact time

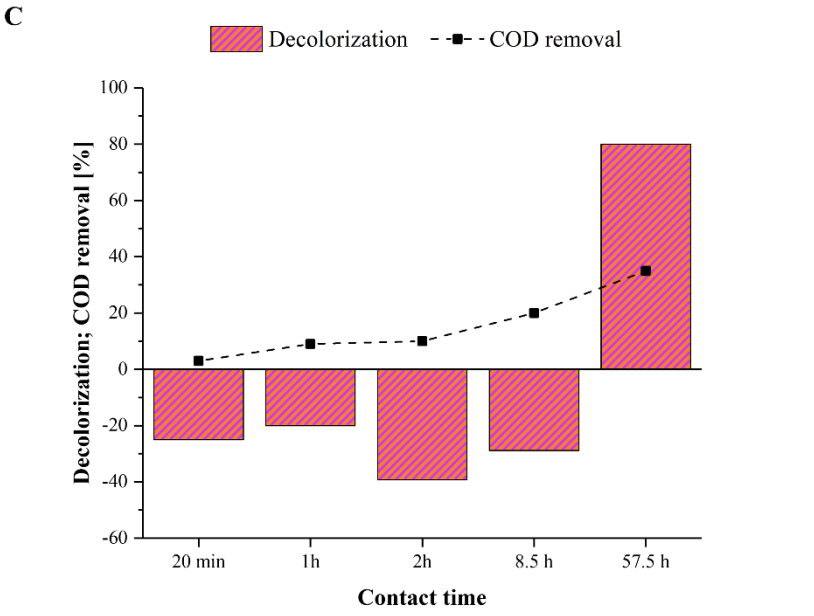
C
Decolorization
COD removal
Decolorization; COD removal [%]
100
80
60
40
20
0
-20
-40
-60
20 min
1h
2h
8.5 h
57.5 h
Contact time

332

Figure 6: *Chemical oxidation of the IWW by single-step dosage in H_2O_2 and UV/H_2O_2 tests (pH= 8; E= 11 mS/cm). Dosage was done at t=0. (**A**) Absorbance at 254 nm and (**B**) decolorization of the IWW as a function of contact time in H_2O_2 tests (H_2O_2= (a) 50 mg L^{-1}, (b) 200 mg L^{-1}, (c) 500 mg L^{-1}, (d) 1500 mg L^{-1} and (e) 3000 mg L^{-1}); (**C**) Decolorization and COD removal in UV/H_2O_2 tests (H_2O_2= 1500 mg L^{-1}). (COLOR online only) (2-column fitting image).*

3.3. H_2O_2-assisted photoelectrocatalysis

There is a wide agreement in literature on the advantages given by combining several techniques for the optimization of decolorization process (Bessegato et al., 2018). Based on the results discussed in the previous sections, the combined H_2O_2-PEC process was investigated. The overall H_2O_2 dosage was 1500 mg L^{-1} considering a high initial COD concentration in the untreated IWW of 1800 mg L^{-1} (H_2O_2 $COD_{initial}^{-1}$ ratio= 0.8). In dosing H_2O_2 two different procedures were followed: (a) single-step mode and (b) three-step mode (500 mg L^{-1} every 40 min). The photoelectrochemical activation of the anodized mesh was monitored by recording the current flowing in the reactor. As previously mentioned, higher currents correspond to higher production of $OH^{\bullet}$ radicals. In Figure 7 the residual H_2O_2 concentration, the absorbance of the IWW at 254 nm and the current flowing in the reactor are represented as a function of the contact time during a PEC test. In general, there is a strong correlation between H_2O_2 dosage and current. Figure 7A clearly shows that within 40 min of contact time the addition of H_2O_2 by single-step dosage corresponded to a significant decrease of IWW absorbance and to an increase of the current up to 79 mA. Qualitatively, a similar behavior was observed by multiple-step dosage (Figure 7B). However, in the latter case, the overall process was slower. In fact, the average current was lower and the absorbance of the IWW higher. Data in Figure 7 also show the absence of light-scavenging effects due to formation of by-products, caused by H_2O_2 addiction. In fact, in both cases, when the H_2O_2 is dosed, the current increased; therefore, this means that the TiO_2 mesh is more effectively activated after H_2O_2 addition. Comparing the currents flowing in the reactor during PEC with and without H_2O_2 addition, it can be argued about the role of H_2O_2 itself. In fact, not only the current increased with H_2O_2 dosage (Figure 7A) but the steady state value was higher by a factor of 2 with respect to PEC alone. This means that in H_2O_2-assisted PEC the catalyst photoactivation was not only anticipated but also enhanced with respect to PEC alone. Therefore, H_2O_2 performed three functions: (i) it decreased the AB_{254} of IWW thus stimulating the activation of the catalyst, (ii) it accepted a photogenerated electrons delivered at the cathode surface to form $OH^{\bullet}$ radical (Eq. 7) and (iii) it formed $OH^{\bullet}$ radicals by reacting with O_2^{-}according to Eq. 8 (Elmolla and Chaudhuri, 2010; Hirakawa and Nosaka, 2002).

$$H_2O_2 + e^- \rightarrow OH^{\cdot} + OH^- \qquad (7)$$

$$H_2O_2 + O_2^{\cdot -} \rightarrow OH^{\cdot} + OH^- + O_2 \quad (8)$$

Therefore, the production rate of $OH^{\bullet}$ increased significantly with the addition of H_2O_2. These results were confirmed in literature by Elmolla and Chaudhuri (2010) and Hirakawa and Nosaka (2002).

In Figure 8, the relative percentage decolorization during H_2O_2-assisted PEC is represented as a function of contact time. Despite the treatment with H_2O_2 alone and UV/H_2O_2 gave color recrudescence within the first 60 min of contact time (Figure 6B-6C), during H_2O_2-assisted PEC recoloration was not detected. Conversely, the dosage mode greatly affected the color and COD removal rate. After a contact time of 20 min single and multiple-step dosing lead to a color removal of 34 % and 8 %, respectively; after 2h, by single-step and multiple-step dosage, the color removal was 55 % and 44 % respectively. Therefore, it can be concluded that single-step dosage is induces a faster decolorization with respect to a three-step dosage. The corresponding COD values reported in Table 3 remained at relatively lower values (24 % and 10 % respectively), confirming the distinction between decolorization and degradation, also reported by Hao et al. (2000). In other terms, these COD values confirm that only a small part of COD of the IWW was due to chromophore-containing molecules.

By comparing the decolorization trend during PEC (Figure 4) and during H_2O_2-assited PEC (Figure 8), in the latter case a much higher color removal rate was observed. For instance, by H_2O_2-assisted PEC (single-step dosage) a relative percentage decolorization of about 55% was obtained after 120 min (Figure 8), without dosing H_2O_2 the same decolorization was obtained in about 3000 min. Since after 20 min the residual concentration of H_2O_2 was below 80 mg L^{-1}, suggesting a negligible oxidation activity, the long-term impact on the PEC process suggests a synergistic effect between H_2O_2 and PEC. This would deserve a deeper understanding, which is out of the scope of the present paper.

After 2 h, H_2O_2-assisted PEC also increased significantly the potential treatability of the IWW by a biological process (Figure 9). In fact, considering both the SOUR and the COD values, it can be inferred that H_2O_2-assisted PEC (single-step dosage) induced the more significant increase on biodegradability of the treated IWW with respect to the other processes. Correspondingly, a much lower effect on biodegradability was obtained by UV.

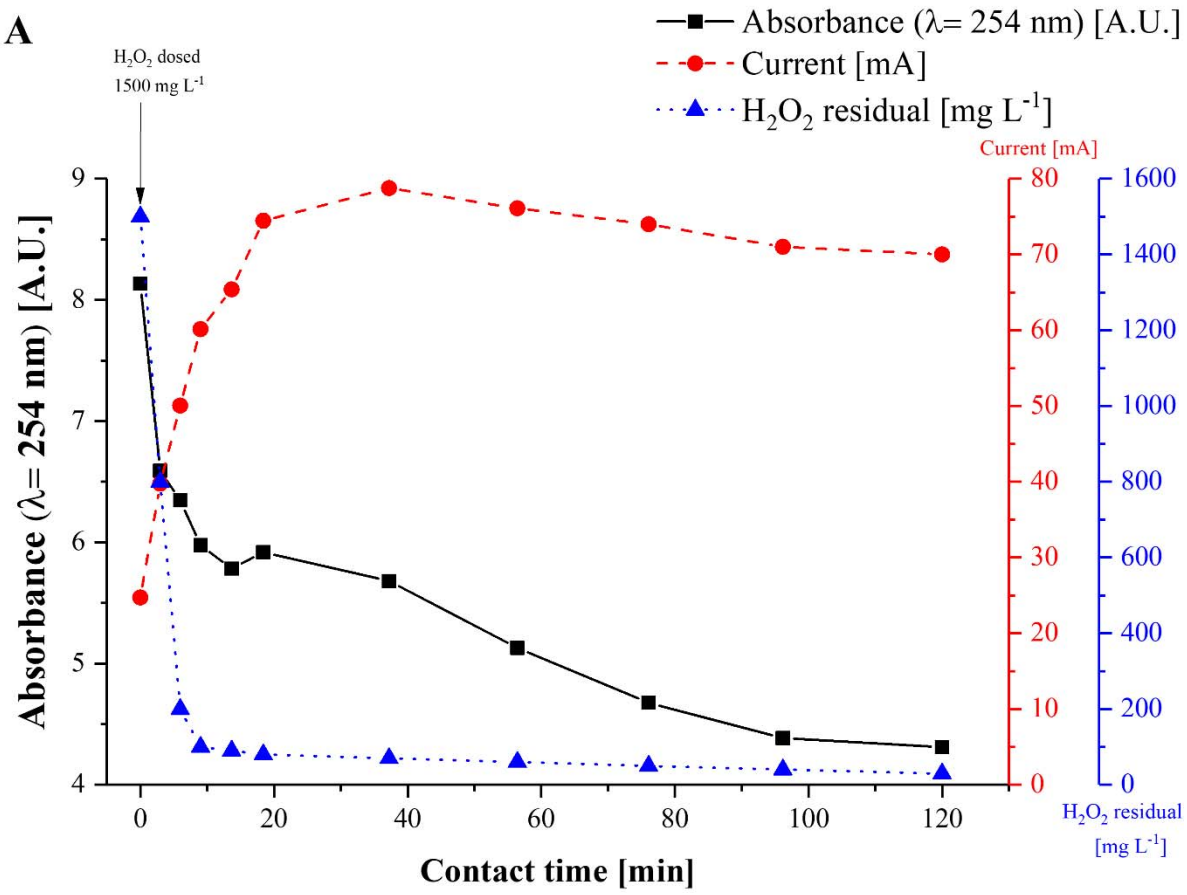
A
Absorbance (λ= 254 nm) [A.U.]
Current [mA]
H2O2 residual [mg L-1]
H2O2 dosed
1500 mg L-1
Absorbance (λ= 254 nm) [A.U.]
Current [mA]
H2O2 residual
[mg L-1]
Contact time [min]

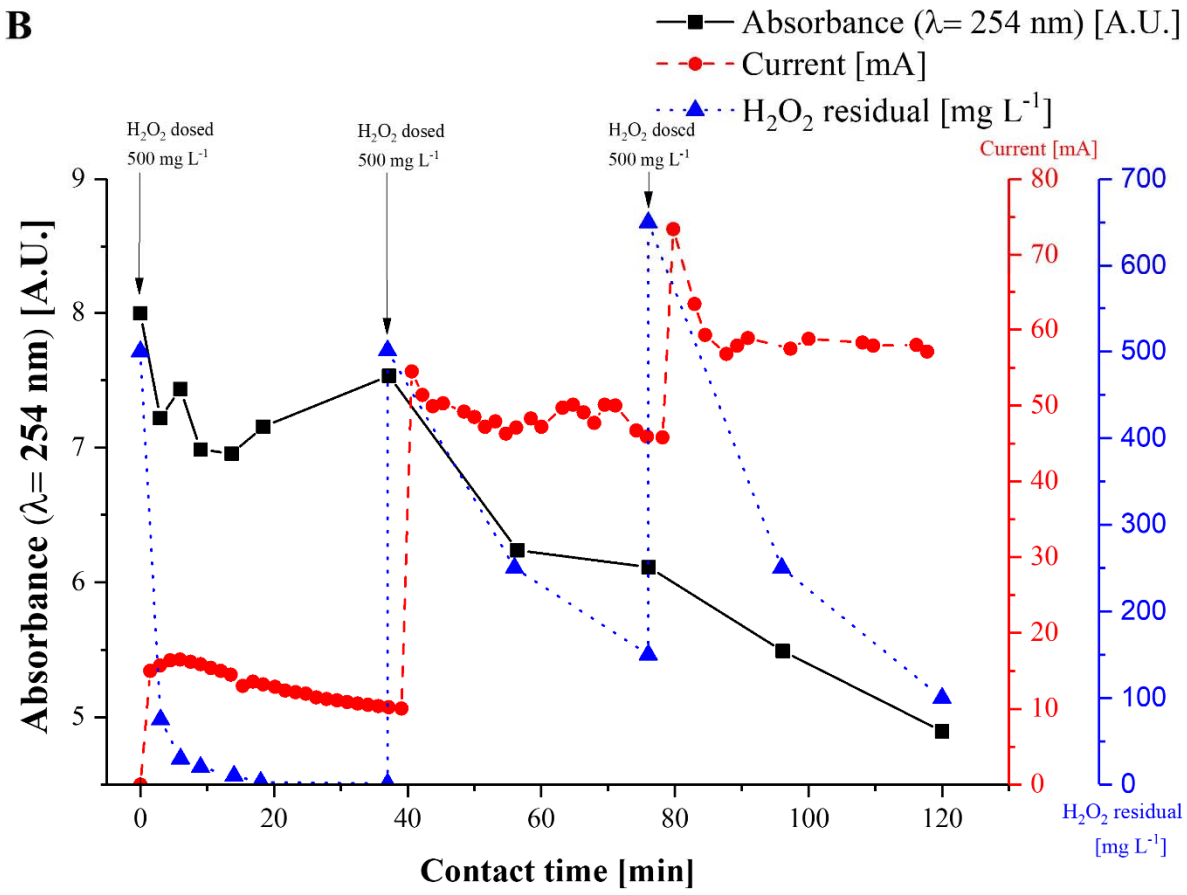
B
Absorbance (λ= 254 nm) [A.U.]
Current [mA]
H2O2 residual [mg L-1]
H2O2 dosed
500 mg L-1
H2O2 dosed
500 mg L-1
H2O2 dosed
500 mg L-1
Absorbance (λ= 254 nm) [A.U.]
Current [mA]
H2O2 residual
[mg L-1]
Contact time [min]

385

386 ***Figure 7:*** *Absorbance at 254 nm, current flowing in the reactor and H_2O_2 residual during H_2O_2-assisted PEC:* ***(A)*** *single*

387 *step dosage.* ***(B)*** *3-steps dosage. (COLOR online only) (single column fitting image)*

388

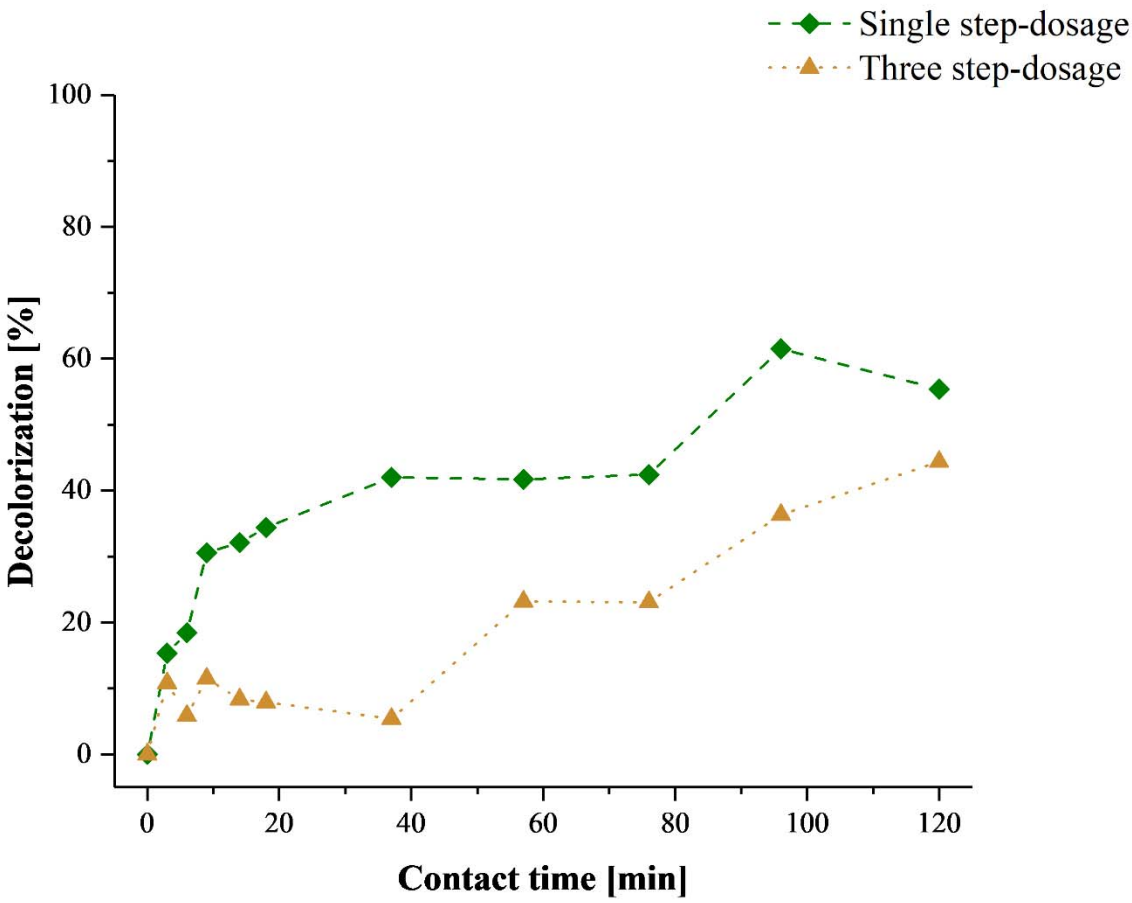

389

390 ***Figure 8:*** *Relative percentage decolorization of the IWW during H_2O_2-assisted PEC (H_2O_2 dosage= 1500 mg L^{-1}).*

391 *(COLOR online only) (single column fitting image)*

392 ***Table 3:*** *Decolorization and COD removal after H_2O_2-assisted PEC processes with single-step dosage and three-step*

393 *dosage as a function of the contact time.*

Contact time	H_2O_2-assisted PEC (single step dosage)	H_2O_2-assisted PEC (three-step dosage)

	Decolorization [%]	COD removal [%]	Decolorization [%]	COD removal [%]
20 min	34.4	19.6	7.9	4.9
1 h	41.7	11.5	23.2	6.7
2 h	55.4	23.6	44.4	9.9

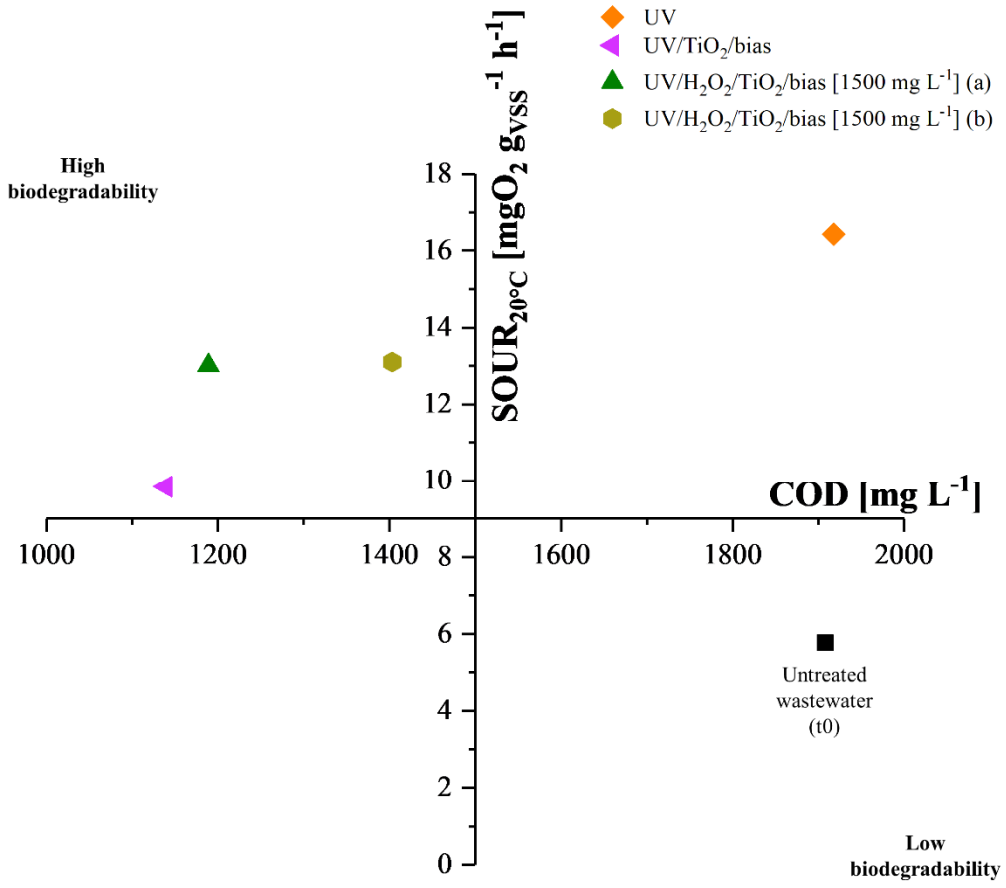

Figure 9: *SOUR values after 2h of H_2O_2-assisted PEC processes (single-step (a) and three-step (b) H_2O_2 dosage) and comparison with SOUR values after 2h of PEC and UV. (COLOR online only) (single column fitting image)*

3.4. Energy consumption

Evaluation of the viability of the process depends on several aspects. These include for example effluent quality goals, maturity of scientific knowledge on the process and economic issues (Cardoso et al., 2016). As reported by Bessegato et

al. (2018), economic aspect due to energy consumption generally represents one of the main operation costs for treatment of IWW by AOPs, particularly for electrochemical processes. Considering that PEC combined with H_2O_2 proved to be the best treatment for the color removal from this IWW, two different energy consumption analysis were carried out. In Figure 10A, values of Electrical energy per unit of mass (E_{EM} kW h Kg^{-1}) after 20 min ad 2h of contact time (respectively 1h and 6h of processing time) with single-step dosage and three-steps dosage of H_2O_2 are compared with COD removal efficiency. The results demonstrate that the three-step dosing required higher energy consumption (up to 1840 kW h Kg^{-1}).

The value of E_{EM} obtained mainly depend on pump power consumption. In fact, considering only the values of the operation of UV and bias, E_{EM} of PEC combined with impulse dosage of H_2O_2 after 2h of contact time (best COD removal) is almost 145 kW h Kg^{-1}.

Moreover, values of Electrical energy per order (E_{EO} kW m^{-3} $order^{-1}$) with the two different H_2O_2 dosage modes are compared with color removal yields (Figure 10B). For both the examined contact time, single-step dosage represents the best solution for optimizing energy consumption. The lowest value of E_{EO} (176.7 kW m^{-3} $order^{-1}$) was obtained 20 min after single-dosage and corresponded to a decolorization yield of 34.4 %.

Data in Figure 10 also highlight the obvious correlation between processing time and electrical energy consumption, which was mainly due to the power consumption of the pump needed to recirculate the IWW. If only UV lamp and bias power consumption are considered, after 2h of contact time (best decolorization) and following single-step dosed H_2O_2, E_{EO} was almost 152 kW m^{-3} $order^{-1}$. Other studies in literature have used this parameter in order to evaluate the costs of different methods of decolorization for real IWW. Values strongly depends on the characteristics of the plant and type of process adopted. For instance, Bessegato et al. (2018) calculated 75 kW m^{-3} $order^{-1}$ for a combined PEC+H_2O_2+O_3 treatment and after a contact time of 30 min. In the present study a very similar outcome was reached after contact time of 20 min by means of the combined process consisting in PEC+H_2O_2, whose E_{EO} was about 50 kW m^{-3} $order^{-1}$.

Considering these results, the higher of energy consumption is due to the pump (72.5%). Therefore, in the perspective of a full-scale application and in order to reduce/eliminate pump energy costs, the design of the PEC apparatus should be reconsidered.

It must be taken into consideration that the H_2O_2 assisted-PEC process also involved the consumption of chemical reagents. However, photolysis assisted with the same quantity of H_2O_2, without the use of TiO_2 and bias, did not provide

any decolorization or COD removal in 2h of contact time (Figure 6C). Moreover, another consideration can be made about the cost related to the use of the bias. The impact of the bias on the energy costs in H_2O_2-assisted PEC can be considered negligible (around 0.3% of the total energy required). As for the cost of the electrode, since this is not a commercial product it is difficult to evaluate a possible cost. However, since the electrode was obtained by an industrial technique already in use in the industry of Al and Mg surface treatments, it is reasonable to expect that an affordable commercial product would be available in case wide industrial application. Furthermore, literature shows that the electrode can be used several times and re-activated if necessary (Murgolo et al., 2019).

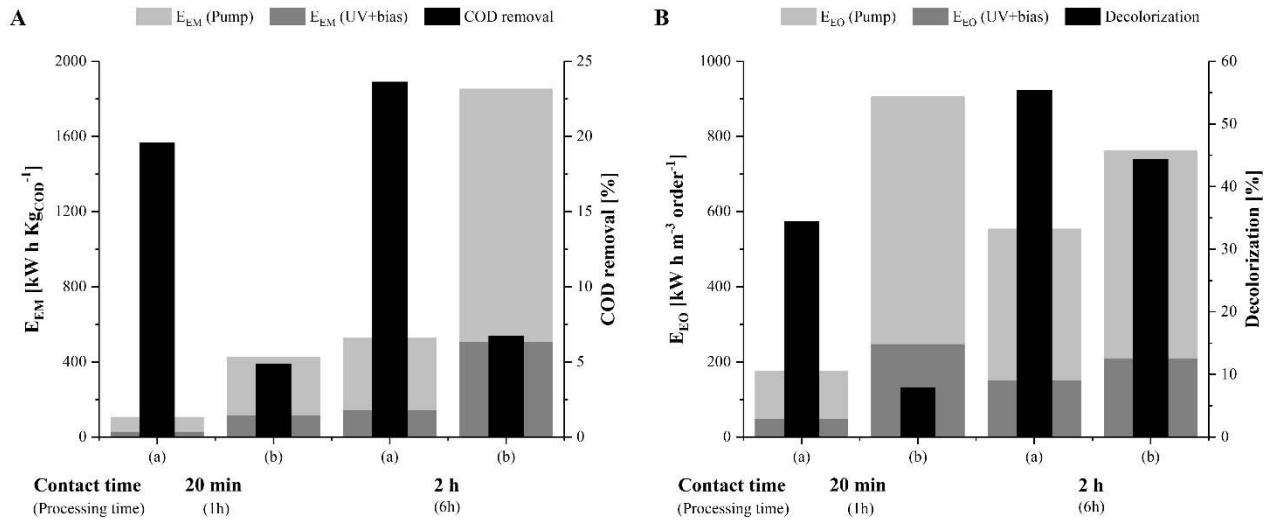

Figure 10: *(**A**) Values of Electrical energy per unit of mass (E_{EM} kW h Kg^{-1}) after 20 min and 2h (contact time) of UV/H_2O_2/TiO_2/bias process with (a) single-step dosage and (b) three-steps dosage of H_2O_2 in comparison with COD removal efficiency. (**B**) Values of Electrical energy per order (E_{EO} kW m^{-3} $order^{-1}$) after 20 min ad 2h (contact time) of UV/H_2O_2/TiO_2/bias process with (a) single-step dosage and (b) three-steps dosage of H_2O_2 in comparison with decolorization efficiency. E_{EM} (Pump) is related to pump power consumption; E_{EM} (UV + bias) is related to UV and bias power consumption. (COLOR online only) (2-column fitting image).*

4. Conclusions

The decolorization of a real pharmaceutical IWW presenting a recalcitrant coloration was accomplished by conventional treatments (photolysis and hydrogen peroxide) and photoelectrocatalytic processes such as UV/TiO_2/Bias and UV/H_2O_2/TiO_2/Bias. Among the considered treatments, the combination of PEC and hydrogen peroxide dosage was demonstrated to be the most effective and fast in decolorization. Two different H_2O_2 dosage modes were tested: (i) single-

step dosing and (ii) three-step dosing. The two dosage modes corresponded respectively to 55 % and 44 % of decolorization after only 2 h of contact time. Although the other processes considered in this study demonstrated the ability to significantly increase the biodegradability of the initial matrix, they were not able to effectively decolorate the IWW in a short time. In fact, photolysis, UV/H_2O_2 and PEC processes lead to a significant color removal (76%, 80% and 86%, respectively) only after a much longer contact time (57.5 h). As for the other parameters analyzed, the COD was in some cases removed quite well (UV/TiO_2/Bias: -42 % after 57.5h of contact time; UV/H_2O_2: -35 % after 57.5h of contact time; UV/H_2O_2/TiO_2/Bias: -24 % after 2h of contact time) demonstrating the difference between decolorization and degradation. Considering the results obtained in terms of decolorization and COD removal, the energy consumption analysis demonstrated that PEC combined with the single-step dosage of H_2O_2 optimizes energy cost. However, in the perspective of a full-scale application and in order to reduce\eliminate pump energy costs, the design of the PEC laboratory scale plant should be optimized.

Acknowledgments

The authors acknowledge Prof. Mariangela Longhi, Department of Chemistry, University of Milano, for the BET tests. The authors also acknowledge Idroclean S.p.A. (Casirate d'Adda, Bergamo, Italy) and ASMortara S.p.A. (Mortara, Pavia, Italy) for giving the financial and technical support to the experimental research.

Declaration of competing interest

None

Funding:

This research did not receive any specific grant from funding agencies in the public, commercial, or not-for-profit sectors.

References

Andronic, L., Isac, L., Miralles-Cuevas, S., Visa, M., Oller, I., Duta, A., Malato, S., 2016. Pilot-plant evaluation of TiO2 and TiO2-based hybrid photocatalysts for solar treatment of polluted water. J. Hazard. Mater. 320, 469–478. https://doi.org/10.1016/j.jhazmat.2016.08.013

APHA, 2012. Standard Methods for the Examination of Water and Wastewater, 22nd Editi. ed, American Public Health Association, American Water Works Association, Water Environment Federation.

Arslan, I., Balcioglu, I.A., Tuhkanen, T., Bahnemann, D., 2000. H_2O_2/UV-C and Fe^{2+}/ H_2O_2/UV-C versus TiO_2/UV-A Treatment for Reactive Dye Wastewater. J. Environ. Eng. 126, 903–911. https://doi.org/10.1061/(ASCE)0733-9372(2000)126:10(903)

Asif, M.B., Hai, F.I., Singh, L., Price, W.E., Nghiem, L.D., 2017. Degradation of Pharmaceuticals and Personal Care Products by White-Rot Fungi—a Critical Review. Curr. Pollut. Reports 3, 88–103. https://doi.org/10.1007/s40726-017-0049-5

Bessegato, G.G., de Souza, J.C., Cardoso, J.C., Zanoni, M.V.B., 2018. Assessment of several advanced oxidation processes applied in the treatment of environmental concern constituents from a real hair dye wastewater. J. Environ. Chem. Eng. 6, 2794–2802. https://doi.org/10.1016/j.jece.2018.04.041

Bestetti, M., Franz, S., Cuzzolin, M., Arosio, P., Cavallotti, P.L., 2007. Structure of nanotubular titanium oxide templates prepared by electrochemical anodization in H2SO4/HF solutions. Thin Solid Films 515, 5253–5258. https://doi.org/10.1016/j.tsf.2006.12.180

Bolton, J.R., Bircher, K.G., Tumas, W., Tolman, C.A., 2001. Figures-of-merit for the technical development and application of advanced oxidation technologies for both electric- and solar-driven systems (IUPAC Technical Report). Pure Appl. Chem. 73, 627–637. https://doi.org/10.1351/pac200173040627

Cardoso, J.C., Bessegato, G.G., Boldrin Zanoni, M.V., 2016. Efficiency comparison of ozonation, photolysis, photocatalysis and photoelectrocatalysis methods in real textile wastewater decolorization. Water Res. 98, 39–46. https://doi.org/10.1016/j.watres.2016.04.004

Cates, E.L., 2017. Photocatalytic Water Treatment: So Where Are We Going with This? Environ. Sci. Technol. 51, 757–758. https://doi.org/10.1021/acs.est.6b06035

Collivignarelli, M., Abbà, A., Benigna, I., Sorlini, S., Torretta, V., 2017a. Overview of the Main Disinfection Processes for Wastewater and Drinking Water Treatment Plants. Sustainability 10, 86. https://doi.org/10.3390/su10010086

Collivignarelli, M.C., Abbà, A., Bertanza, G., 2014. Treatment of high strength pharmaceutical wastewaters in a Thermophilic Aerobic Membrane Reactor (TAMR). Water Res. 63, 190–198. https://doi.org/10.1016/j.watres.2014.06.018

Collivignarelli, M.C., Abbà, A., Bertanza, G., Barbieri, G., 2017b. Treatment of high strength aqueous wastes in a

498 thermophilic aerobic membrane reactor (TAMR): performance and resilience. Water Sci. Technol. 76, 3236–
499 3245. https://doi.org/10.2166/wst.2017.492

500 Collivignarelli, M.C., Abbà, A., Bestetti, M., Crotti, B.M., Carnevale Miino, M., 2019a. Electrolytic Recovery of Nickel
501 and Copper from Acid Pickling Solutions Used to Treat Metal Surfaces. Water, Air, Soil Pollut. 230, 101.
502 https://doi.org/10.1007/s11270-019-4158-1

503 Collivignarelli, M.C., Abbà, A., Carnevale Miino, M., Damiani, S., 2019b. Treatments for color removal from
504 wastewater: State of the art. J. Environ. Manage. 236. https://doi.org/10.1016/j.jenvman.2018.11.094

505 Collivignarelli, M.C., Abbà, A., Carnevale Miino, M., Torretta, V., 2019c. What Advanced Treatments Can Be Used to
506 Minimize the Production of Sewage Sludge in WWTPs? Appl. Sci. 9, 2650. https://doi.org/10.3390/app9132650

507 Collivignarelli, M.C., Bertanza, G., Abbà, A., Torretta, V., Katsoyiannis, I.A., 2019c. Wastewater treatment by means
508 of thermophilic aerobic membrane reactors: respirometric tests and numerical models for the determination of
509 stoichiometric/kinetic parameters. Environ. Technol. 40, 182–191.
510 https://doi.org/10.1080/09593330.2017.1384070

511 Collivignarelli, M.C., Canato, M., Abbà, A., Marco, C.M., 2019d. Biosolids: what are the different types of reuse? J.
512 Clean. Prod. 117844. https://doi.org/10.1016/j.jclepro.2019.117844

513 Cui, W., He, J., Wang, H., Hu, J., Liu, L., Liang, Y., 2018. Polyaniline hybridization promotes photo-electro-catalytic
514 removal of organic contaminants over 3D network structure of rGH-PANI/TiO2 hydrogel. Appl. Catal. B
515 Environ. 232, 232–245. https://doi.org/10.1016/j.apcatb.2018.03.069

516 Del Moro, G., Mancini, A., Mascolo, G., Di Iaconi, C., 2013. Comparison of UV/H2O2 based AOP as an end treatment
517 or integrated with biological degradation for treating landfill leachates. Chem. Eng. J. 218, 133–137.
518 https://doi.org/10.1016/j.cej.2012.12.086

519 Del Moro, G., Prieto-Rodríguez, L., De Sanctis, M., Di Iaconi, C., Malato, S., Mascolo, G., 2016. Landfill leachate
520 treatment: Comparison of standalone electrochemical degradation and combined with a novel biofilter. Chem.
521 Eng. J. 288, 87–98. https://doi.org/10.1016/j.cej.2015.11.069

522 Dotto, J., Fagundes-Klen, M.R., Veit, M.T., Palácio, S.M., Bergamasco, R., 2019. Performance of different coagulants
523 in the coagulation/flocculation process of textile wastewater. J. Clean. Prod. 208, 656–665.

524 https://doi.org/10.1016/j.jclepro.2018.10.112

525 Franz, S., Perego, D., Marchese, O., Bestetti, M., 2015. Photoelectrochemical advanced oxidation processes on
526 nanostructured TiO_2 catalysts: Decolorization of a textile azo-dye. J. Water Chem. Technol. 37, 108–115.
527 https://doi.org/10.3103/S1063455X15030029

528 Franz, S., Perego, D., Marchese, O., Lucotti, A., Bestetti, M., 2016. Photoactive TiO_2 coatings obtained by Plasma
529 Electrolytic Oxidation in refrigerated electrolytes. Appl. Surf. Sci. 385, 498–505.
530 https://doi.org/10.1016/j.apsusc.2016.05.032

531 Freeling, F., Alygizakis, N.A., von der Ohe, P., Slobodnik, J., Oswald, P., Aalizadeh, R., Cirka, L., Thomaidis, N.S.,
532 Scheurer, M., 2019. Occurrence and potential environmental risk of surfactants and their transformation products
533 discharged by wastewater treatment plants. Sci. Total Environ. https://doi.org/10.1016/j.scitotenv.2019.04.445

534 Fujimoto, Y., 1964. Graphical use of first-stage BOD equation. J. Water Pollut. Control Fed. 69–71.

535 Garcia, J., Oliveira, J., Silva, A., Oliveira, C., Nozaki, J., Desouza, N., 2007. Comparative study of the degradation of
536 real textile effluents by photocatalytic reactions involving UV/TiO2/H2O2 and UV/Fe2+/H2O2 systems. J.
537 Hazard. Mater. 147, 105–110. https://doi.org/10.1016/j.jhazmat.2006.12.053

538 Garcia-Segura, S., Brillas, E., 2017. Applied photoelectrocatalysis on the degradation of organic pollutants in
539 wastewaters. J. Photochem. Photobiol. C Photochem. Rev. 31, 1–35.
540 https://doi.org/10.1016/j.jphotochemrev.2017.01.005

541 Ghalebizade, M., Ayati, B., 2016. Solar photoelectrocatalytic degradation of Acid Orange 7 with ZnO/TiO_2
542 nanocomposite coated on stainless steel electrode. Process Saf. Environ. Prot. 103, 192–202.
543 https://doi.org/10.1016/j.psep.2016.07.009

544 Gotovtsev, A. V., 2016. Evaluating BOD and the coefficient of oxidation rate: Monitoring, direct and inverse problems,
545 formulas, calculations and tables. Water Resour. 43, 885–898. https://doi.org/10.1134/S0097807816050067

546 Hagman, M., La Cour Jansen, J., 2007. Oxygen uptake rate measurements for application at wastewater treatment
547 plants. Vatten 63, 131–138.

548 Hao, O.J., Kim, H., Chiang, P.-C., 2000. Decolorization of Wastewater. Crit. Rev. Environ. Sci. Technol. 30, 449–505.

549 https://doi.org/10.1080/10643380091184237

550 Hirakawa, T., Nosaka, Y., 2002. Properties of $O_2^{\bullet-}$ and OH• Formed in TiO_2 Aqueous Suspensions by Photocatalytic
551 Reaction and the Influence of H_2O_2 and Some Ions. Langmuir 18, 3247–3254. https://doi.org/10.1021/la015685a

552 Hou, Y., Qu, J., Zhao, X., Lei, P., Wan, D., Huang, C.P., 2009. Electro-photocatalytic degradation of acid orange II
553 using a novel TiO_2/ACF photoanode. Sci. Total Environ. 407, 2431–2439.
554 https://doi.org/10.1016/j.scitotenv.2008.12.055

555 ISO 8192, 2007. Water Quality - Test for inhibition of oxygen consumption by activated sludge for carbonaceous and
556 ammonium oxidation.

557 Komtchou, S., Dirany, A., Drogui, P., Delegan, N., El Khakani, M.A., Robert, D., Lafrance, P., 2016. Degradation of
558 atrazine in aqueous solution with electrophotocatalytic process using TiO_{2-x} photoanode. Chemosphere 157, 79–
559 88. https://doi.org/10.1016/j.chemosphere.2016.05.022

560 Liu, Y., Zhu, L., 2017. Enhanced treatment of dispersed dye-production wastewater by self-assembled organobentonite
561 in a one-step process with poly-aluminium chloride. Sci. Rep. 7, 6843. https://doi.org/10.1038/s41598-017-
562 07333-2

563 Nakata, K., Fujishima, A., 2012. TiO2 photocatalysis: Design and applications. J. Photochem. Photobiol. C Photochem.
564 Rev. 13, 169–189. https://doi.org/10.1016/j.jphotochemrev.2012.06.001

565 Maiti, S., Sinha, S.S., Singh, M., 2017. Microbial decolorization and detoxification of emerging environmental
566 pollutant: Cosmetic hair dyes. J. Hazard. Mater. 338, 356–363. https://doi.org/10.1016/j.jhazmat.2017.05.034

567 Malpass, G.R.P., Miwa, D.W., Mortari, D.A., Machado, S.A.S., Motheo, A.J., 2007. Decolorisation of real textile waste
568 using electrochemical techniques: Effect of the chloride concentration. Water Res. 41, 2969–2977.
569 https://doi.org/10.1016/j.watres.2007.02.054

570 Mashkoor, F., Nasar, A., Inamuddin, Asiri, A.M., 2018. Exploring the Reusability of Synthetically Contaminated
571 Wastewater Containing Crystal Violet Dye using Tectona grandis Sawdust as a Very Low-Cost Adsorbent. Sci.
572 Rep. 8, 8314. https://doi.org/10.1038/s41598-018-26655-3

573 Mirelman, L.K., Curran, J.A., Clyne, T.W., 2012. The production of anatase-rich photoactive coatings by plasma

574 electrolytic oxidation. Surf. Coatings Technol. 207, 66–71. https://doi.org/10.1016/j.surfcoat.2012.05.076

575 Murgolo, S., Franz, S., Arab, H., Bestetti, M., Falletta, E., Mascolo, G., 2019. Degradation of emerging organic
576 pollutants in wastewater effluents by electrochemical photocatalysis on nanostructured TiO_2 meshes. Water Res.
577 164, 114920. https://doi.org/10.1016/j.watres.2019.114920

578 Murgolo, S., Yargeau, V., Gerbasi, R., Visentin, F., El Habra, N., Ricco, G., Lacchetti, I., Carere, M., Curri, M.L.,
579 Mascolo, G., 2017. A new supported TiO_2 film deposited on stainless steel for the photocatalytic degradation of
580 contaminants of emerging concern. Chem. Eng. J. 318, 103–111. https://doi.org/10.1016/j.cej.2016.05.125

581 Nurhayati, E., 2016. Electro-photocatalytic Fenton Decolorization of Orange G Using Mesoporous TiO_2/stainless Steel
582 Mesh Photo-Electrode Prepared by the Sol-Gel Dip-Coating Method. Int. J. Electrochem. Sci. 3615–3632.
583 https://doi.org/10.20964/110346

584 Oke, I.A., Lukman, S., Amoko, J.S., Fehintola, E.O., 2018. An evaluation of solutions to moment method of
585 biochemical oxygen demand kinetics. Niger. J. Technol. 37, 1. https://doi.org/10.4314/njt.v37i1.1

586 Robinson, T., McMullan, G., Marchant, R., Nigam, P., 2001. Remediation of dyes in textile effluent: a critical review
587 on current treatment technologies with a proposed alternative. Bioresour. Technol. 77, 247–255.
588 https://doi.org/10.1016/S0960-8524(00)00080-8

589 Roy, U., Manna, S., Sengupta, S., Das, P., Datta, S., Mukhopadhyay, A., Bhowal, A., 2018. Dye Removal Using
590 Microbial Biosorbents, in: Green Adsorbents for Pollutant Removal. pp. 253–280. https://doi.org/10.1007/978-3-
591 319-92162-4_8

592 Spurr, R.A., Myers, H., 1957. Quantitative Analysis of Anatase-Rutile Mixtures with an X-Ray Diffractometer. Anal.
593 Chem. 29, 760–762. https://doi.org/10.1021/ac60125a006

594 Stasinakis, A.S., 2013. Use of selected advanced oxidation processes (AOPs) for wastewater treatment - a mini review.
595 Glob. NEST J. 10, 376–385. https://doi.org/10.30955/gnj.000598

596 Stefan, M.I., 2018. UV/hydrogen peroxide process, in: Advanced Oxidation Processes for Water Treatment:
597 Fundamentals and Applications. IWA Publishing, London, pp. 7–122.

598 Suhadolnik, L., Pohar, A., Novak, U., Likozar, B., Mihelič, A., Čeh, M., 2019. Continuous photocatalytic,

599 electrocatalytic and photo-electrocatalytic degradation of a reactive textile dye for wastewater-treatment
600 processes: Batch, microreactor and scaled-up operation. J. Ind. Eng. Chem. 72, 178–188.
601 https://doi.org/10.1016/j.jiec.2018.12.017

602 Trasatti, S., Petrii, O.A., 1992. Real surface area measurements in electrochemistry. J. Electroanal. Chem. 327, 353–
603 376. https://doi.org/10.1016/0022-0728(92)80162-W

604 Turolla, A., Fumagalli, M., Bestetti, M., Antonelli, M., 2012. Electrophotocatalytic decolorization of an azo dye on
605 TiO_2 self-organized nanotubes in a laboratory scale reactor. Desalination 285, 377–382.
606 https://doi.org/10.1016/j.desal.2011.10.029

607 Wang, K., Chen, H.-Y., Huang, L.-C., Su, Y.-C., Chang, S.-H., 2008. Degradation of Reactive Black 5 using combined
608 electrochemical degradation-solar-light/immobilized TiO2 film process and toxicity evaluation. Chemosphere 72,
609 299–305. https://doi.org/10.1016/j.chemosphere.2008.02.012

610 Wang, H., Liang, Y., Liu, L., Hu, J., Cui, W., 2018. Highly ordered TiO2 nanotube arrays wrapped with g-C3N4
611 nanoparticles for efficient charge separation and increased photoelectrocatalytic degradation of phenol. J. Hazard.
612 Mater. 344, 369–380. https://doi.org/10.1016/j.jhazmat.2017.10.044

613 Wang, H., Liang, Y., Liu, L., Hu, J., Wu, P., Cui, W., 2017. Enriched photoelectrocatalytic degradation and photoelectric
614 performance of BiOI photoelectrode by coupling rGO. Appl. Catal. B Environ. 208, 22–34.
615 https://doi.org/10.1016/j.apcatb.2017.02.055

616 Wen, S., Chen, L., Li, W., Ren, H., Li, K., Wu, B., Hu, H., Xu, K., 2018. Insight into the characteristics, removal, and
617 toxicity of effluent organic matter from a pharmaceutical wastewater treatment plant during catalytic ozonation.
618 Sci. Rep. 8, 9581. https://doi.org/10.1038/s41598-018-27921-0

619 Yerokhin, A.L., Nie, X., Leyland, A., Matthews, A., 2000. Characterisation of oxide films produced by plasma electrolytic
620 oxidation of a Ti–6Al–4V alloy. Surf. Coatings Technol. 130, 195–206. https://doi.org/10.1016/S0257-
621 8972(00)00719-2

622 Yerokhin, A.L., Nie, X., Leyland, A., Matthews, A., Dowey, S.J., 1999. Plasma electrolysis for surface engineering. Surf.
623 Coatings Technol. 122, 73–93. https://doi.org/10.1016/S0257-8972(99)00441-7

624 Zhan, J., Li, Z., Yu, G., Pan, X., Wang, J., Zhu, W., Han, X., Wang, Y., 2019. Enhanced treatment of pharmaceutical

625 wastewater by combining three-dimensional electrochemical process with ozonation to in situ regenerate granular
626 activated carbon particle electrodes. Sep. Purif. Technol. 208, 12–18. https://doi.org/10.1016/j.seppur.2018.06.030

627 Zhang, Y., Cui, W., An, W., Liu, L., Liang, Y., Zhu, Y., 2018. Combination of photoelectrocatalysis and adsorption for
628 removal of bisphenol A over TiO2-graphene hydrogel with 3D network structure. Appl. Catal. B Environ. 221, 36–
629 46. https://doi.org/10.1016/j.apcatb.2017.08.076

630 Zhao, J., He, Q., Zhang, X., Guo, X., Song, Q., Liu, Y., Yao, B., Zhang, Q., Dionysiou, D.D., 2019. Fabrication of
631 CQDs/$Bi_5Nb_3O_{15}$ nanocomposites for photocatalytic degradation of veterinary pharmaceutical sarafloxacin. Catal.
632 Today 3, 88–103. https://doi.org/10.1016/j.cattod.2019.05.006

633